Science of the Total Environment 769 (2021) 144706

Contents lists available at ScienceDirect

Science of the Total Environment

journal homepage: www.elsevier.com/locate/scitotenv

Impacts of freeze-thaw processes and subsequent runoff on ^{137}Cs washoff from bare land in Fukushima

Yasunori Igarashi [a], Yuichi Onda [b,*], Yoshifumi Wakiyama [a], Kazuya Yoshimura [c], Hiroaki Kato [b], Shohei Kozuka [d], Ryo Manome [e]

[a] Institute of Environmental Radioactivity, Fukushima University, 1 Kanayagawa, Fukushima-shi, Fukushima, 960-1296, Japan
[b] Department of Integrative Environmental Sciences, Faculty of Life and Environmental Sciences, University of Tsukuba, 1-1-1 A-405 Tennodai, Tsukuba-shi, Ibaraki 305-8572, Japan
[c] Sector of Fukushima Research and Development, Japan Atomic Energy Agency, 45-169 Sukakeba, Kaibana, Haramachi-ku, Minamisoma City, Fukushima 975-0036, Japan
[d] Ministry of the Environment, 1-2-2 Kasumigaseki, Chiyoda-ku, Tokyo 100-8975, Japan
[e] Disaster Prevention Technology Division, Geo-hazard & Risk Mitigation, Railway Technical Research Institute, 2-8-38 Hikari-cho, Kokubunji-shi, Tokyo 185-8540, Japan

HIGHLIGHTS

- ^{137}Cs dynamics and sediment discharge in Fukushima were studied.
- Freeze–thaw processes and rill formation make ^{137}Cs wash-off seasonal.
- Erosion processes must be considered to improve understanding of ^{137}Cs dynamics.

GRAPHICAL ABSTRACT

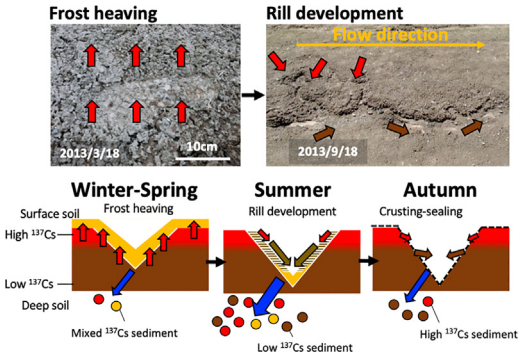

ARTICLE INFO

Article history:
Received 10 August 2020
Received in revised form 18 December 2020
Accepted 21 December 2020
Available online 20 January 2021

Editor: Paulo Pereira

Keywords:
Seasonal sediment transport
^{137}Cs concentration
^{137}Cs wash-off
Soil erosion
Frost-heaving
Freeze-thaw processes

ABSTRACT

The deposited ^{137}Cs is one of the long-lived radionuclides, that was released following the Fukushima Dai-ichi Nuclear Power Plant (FDNPP) accident, has been hydrologically transported as particulates in the terrestrial environment of the Fukushima region. The impact of freeze-thaw processes and subsequent runoff affecting the ^{137}Cs flux and concentration in sediment discharge were revealed in bare land erosion plot following the FDNPP accident by detailed monitoring and laser scanner measurement on the soil surface. We found that surface topographic changes due to the frost-heaving during the winter-spring period, and rill formation during the summer. We also found the evident seasonal changes in ^{137}Cs concentration; high during the early spring and gradually decreased thereafter, then surface runoff from the plot frequently occurred during spring and autumn when rainfall was high and reached a maximum in summer. From these results, the higher ^{137}Cs concentration in spring was caused by a mixture of unstable surface sediment following freeze-thaw processes and then transported in the early spring, but erosion amount is not significant because of the less rainfall event. The sediment with a lower ^{137}Cs concentration, which was supplied from the rill erosion and its expansion, was washoffed during the summer, contributing most of the flux from erosion in bare land in Fukushima region. In case, heavy rainfall occurs in the early spring, caution is required because high concentrations of cesium may flow down into the river.

* Corresponding author.
E-mail addresses: onda@geoenv.tsukuba.ac.jp, y-onda@jc5.so-net.ne.jp (Y. Onda).

https://doi.org/10.1016/j.scitotenv.2020.144706
0048-9697/

1. Introduction

Radionuclide wash-off, which is the transport of flowing water over the soil surface (runoff), can play a significant role in radionuclides transport and redistribution in the environment (Santschi et al., 1988; Santschi et al., 1990; Garcia-Sanchez and Konoplev, 2009; Beresford et al., 2016). The ^{137}Cs is one of the long-lived radionuclides that was released following the accident at Fukushima Dai-ichi Nuclear Power Plant (FDNPP); it poses significant radiological risks, aquatic insects, fish and the in the fresh water aquatic systems (Yoshimura and Akama, 2014 Wada et al., 2016 Steinhauser et al., 2014). Also, the transported radiocesium to the ocean is easy to become dissolved phase due to the chemical compensate with seawater, and dissolved radiocesium in seawater will readily become incorporated in the marine fish food web (Tagami and Uchida, 2016; Takata et al., 2016; Carvalho, 2018). A large amount of ^{137}Cs was transported hydrologically in the terrestrial environment of the Fukushima region, mainly as particulates, after the FDNPP accident (Nagao et al., 2013 Nakao et al., 2014 Taniguchi et al., 2019 Onda et al., 2020). For instance, in total, 12 TBq of ^{137}Cs was transported in the Abukuma River (the largest river system in the area contaminated by the FDNPP accident) to the ocean between June 2011 and August 2015, and almost all (96.5%) of this ^{137}Cs was transported in particulates (Taniguchi et al., 2019). Soil and sediment transport are therefore key to understanding ^{137}Cs dynamics in the Fukushima region.

Radionuclides in the area contaminated by the Chernobyl nuclear power plant accident were thought to have been washed off the soil attached to particulates into rivers and transported in suspended sediment (Santschi et al., 1990 Sansone et al., 1996 Smith and Beresford, 2005). Field experiments after the Chernobyl nuclear power plant accident showed that extreme rainfall could cause marked surface runoff containing dissolved and particulate radionuclides (Bulgakov et al., 1991 Konoplev et al., 1996 Bulgakov et al., 1999 Garcia-Sanchez et al., 2005). In these experiments, surface runoff was measured during the snowmelt season, and the frozen near-surface soil was found to have enhanced radionuclide redistribution through wash-off processes (Konoplev et al., 1992). However, no detailed field evidence is available in this context. Surface wash-off processes have also been investigated in the ^{137}Cs-contaminated area contaminated with ^{137}Cs by the FDNPP accident. In studies conducted between July 2011 and November 2012, clear differences were found in the sediment wash-off and ^{137}Cs fluxes for different land uses. Soil erosion normalized to factors such as rainfall erosivity, soil erodibility, and slope steepness was represented well by an exponential function of vegetation cover, and the highest soil erosion and ^{137}Cs wash-off rates were found for bare uncultivated land (Yoshimura et al., 2015). Wakiyama et al. (2019) reported that plot scale ^{137}Cs wash-off for multiple years implied that a rill development lowered ^{137}Cs concentration in sediment from a bare land plot. On the other hand, they did not address the processes in different seasons. For instance, freezing and thawing of top soil surface develops unstable surface soil by making frost-heaving (freeze-thaw processes) (Arnáez and Larrea, 1995 Arnáez et al., 2004 Bechmann et al., 2005 Nadal-Romero et al., 2008), and can strongly increase soil erosion in early spring and when rain falls. The freeze-thaw process and the subsequent runoff on ^{137}Cs wash-offs are always accompanied by the surface topography changes. Therefore, it is assumed that the microtopography will be useful to identify and quantify the soil surface erosion processes that transport ^{137}Cs to watercourses.

The recently developed terrestrial-laser-scanning (TLS) unmanned aerial vehicle and structure-from-motion method could be used to improve our understanding of soil erosion processes (Eltner and Baumgart, 2015 Eltner et al., 2015) to allow the hydrological aspects of surface runoff and sediment transport on the soil surface to be parameterized (Jester and Klik, 2005). Temporal changes in volumetrically quantified soil surface roughness and rill development were found in the studies mentioned above. Surface changes during winter were caused by crusting and sheet erosion, and changes in the spring rainy season were caused by sheet erosion and rill incision. Understanding surface wash-off caused by overland flow on hillsides is essential when trying to understand hillside–stream runoff and sediment dynamics in headwater catchments. This is particularly important in the more mountainous parts of Japan, which have steeply sloping land (Gomi et al., 2008), receive high precipitation, and suffer high levels of erosion (Laceby et al., 2016). The impacts of seasonal changes in the soil surface could be investigated using the ^{137}Cs concentrations and by performing microtopographic assessments to acquire more information on soil erosion and ^{137}Cs wash-off processes.

Using the TLS technology allows the effects of freezing and thawing of surface soil on microtopographic changes to be monitored (Haubrock et al., 2009). The effects of seasonal changes in surface soil conditions on the erosion process and the consequent scouring of ^{137}Cs can be elucidated. Thus, the aim of this study is to examine the impact of freeze-thaw processes and subsequent runoff on and sediment wash-off and ^{137}Cs concentration by detailed measurement of the microtopography of the soil surface. For this purpose, we conducted continuous measurements of ^{137}Cs wash-off via soil erosion from controlled bare land in the Fukushima area. Soil erosion, ^{137}Cs wash-off, and microtopographic changes were measured using a standard a universal soil-loss equation and data for soil on a plot 5 m wide and 22.13 m long with an adequate length down a slope.

2. Material and method

2.1. Study site

This research was conducted in Yamakiya, Kawamata in Fukushima Prefecture, Japan (37°35′52.8″N, 140°40′26.4″E; Fig. 1a). The slope of the study area was 4.4°. The FDNPP-derived ^{137}Cs fall-out inventory was estimated to be 372 kBq m^{-2} at the study site (Wakiyama et al., 2019 MEXT, 2011). The climate here is classified as the Humid subtropical climate (Cfa) by the Köppen-Geiger system (Peel et al., 2007). Soil type in this plot was classified as reformed soil in Comprehensive Soil Classification System of Japan (Takahashi et al., 2015), and can be classified Cambisol (Transportic) in World Reference Base for Soil Resources (Obara et al., 2011). The site was used as a tobacco-field before the FDNPP accident. The field experiment details are given in Section 2.2. Precipitation was measured at Yamakita station (37°36′03″ N, 140°40′32″ E), 0.2 km from the study site, over a long period (1995–2014). The relevant data were downloaded from the Japanese Ministry of Land, Infrastructure and Transport website (http://www1.river.go.jp/cgi-bin/SiteInfo.exe?ID=102011282218120). Annual precipitation at Yamakita station is 1180 ± 229 mm (mean ± standard deviation). Mean monthly precipitation is highest in September and lowest in February. Rainfall during the study was monitored using an RG200 rain gauge next to the plot (RG200, Global Water Instrumentation, Inc., Gold River, CA, USA). In this study, rainfall measured at the site was used for the analysis (Section 2.3). Since an ambient air temperature from October 2018 to September 2019 had been measured by water/temperature-sensor (Water Height/Temperature Datalogger, Trutrack Inc., Christchurch, New Zealand), the past air temperature was estimated the liner relationship ($y = 0.80\,x + 1.8$; $R^2 = 0.91$) between the site (y) and Iitate meteo-station (x) (37°39′08.0″N, 140°43′06.7″E; 7.3 km from the study site). The Iitate meteo-station data were downloaded from the Japan Meteorological Agency website (http://www.jma.go.jp/jma/index.html). Estimated long-term air temperature (1995–2015) was 10.4 ± 0.4 °C. The highest monthly air temperature was observed in August and the minimum in January.

2.2. Monitoring and measurements of ^{137}Cs

Observations were made on a soil erosion plot installed on uncultivated farmland since 17 July 2011. The USLE was used to monitor surface wash-off events, along with a surface runoff monitoring apparatus at the outlet of the eroding surface and sediment traps (Fig. 1B). In previous

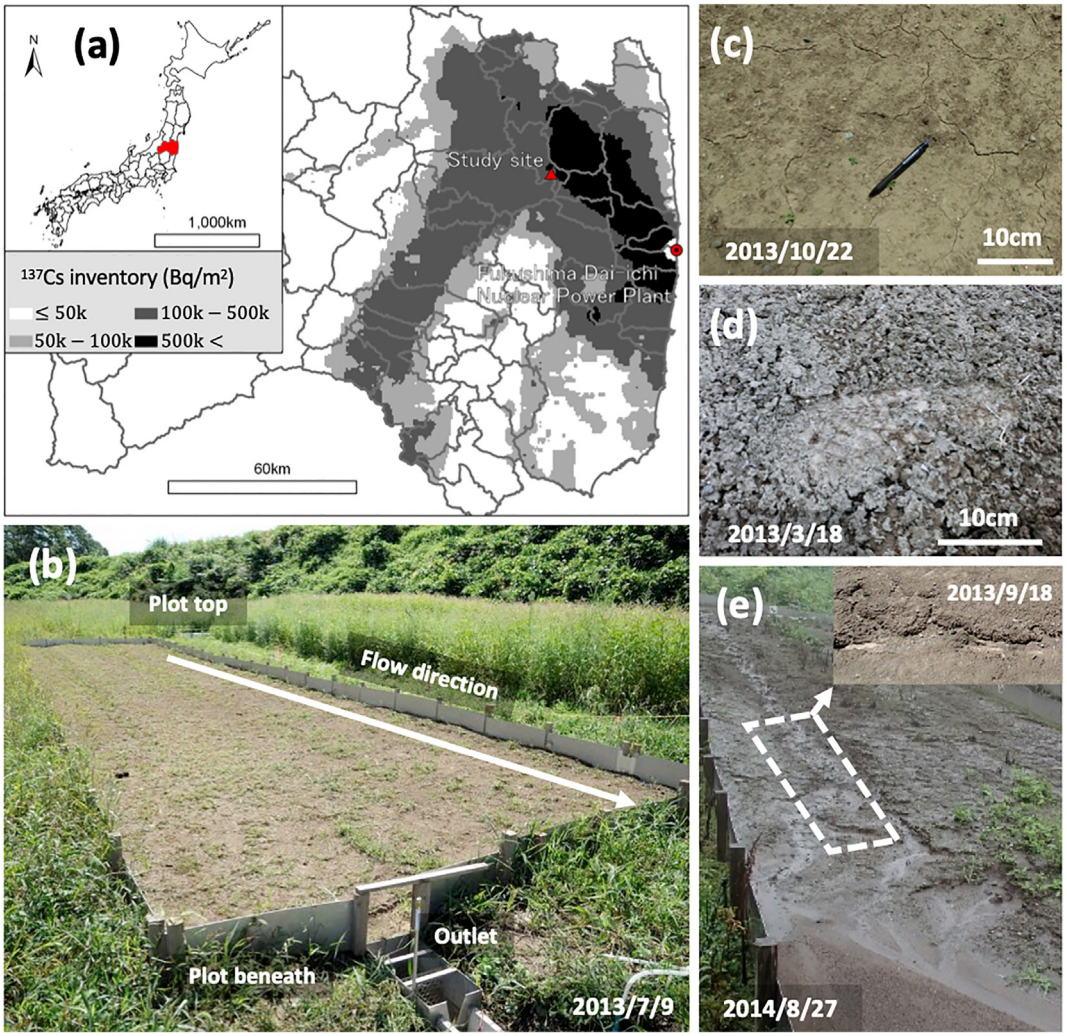

Fig. 1. (a) Map of the study site at which ^{137}Cs deposition was determined in the third airborne survey (MEXT, 2011). (b) Standard universal soil loss equation plot. Examples of typical soil changes: (c) crusting and sealing; (d) frost-heave; and (e) rill formation.

studies, stronger ^{137}Cs wash-off was found for bare land than for land with various types of cover (Yoshimura et al., 2015 Wakiyama et al., 2019). A herbicide was applied to the plot to control vegetation from 13 July 2012. Vegetation cover was controlled with monthly herbicide operations. Water discharges from the site were monitored using a water/temperature-sensor (Water Height/Temperature Datalogger, Trutrack Inc., Christchurch, New Zealand) with a triangular weir (30° V-notch discharge gauge, Tsukahara Manufacturing Co., Ltd., Kyoto, Japan). Eroded soil was trapped in three storage tanks using a multipipe divisor system after the triangular weir. The collected sediment was divided into two components, coarse (deposited) and fine (suspended), in the field. The total amount of eroded soil was defined as the sum of the amounts of coarse and fine soil sediment. The ^{137}Cs concentrations (in Bq kg^{-1}) in the coarse and fine sediment samples were determined by gamma spectrometry. When sufficient material was collected, the particle size distribution was determined using a SALD-3100 laser diffraction particle size analyzer (Shimadzu, Kyoto, Japan). The methods used were described in more detail in previous publications (Yoshimura et al., 2015; Wakiyama et al., 2019).

2.3. Observations of surface topography changes

A three-dimensional (3D) laser scanner was used to make the surface 3D model. A surface survey of the plot was conducted using a Leica Scan Station C5 (Leica Geosystems Co., Ltd., Zurich, Switzerland), which has accuracy for a distance of 4 mm. The surface survey was conducted from several points to avoid shading effects (e.g., from a plot wall, rill or fallows area; Fig. S1). The measured datasets were combined via 6-inch targets (Fig. S2A, B), which were fixed on the plot wall, using the Cyclone 7.4 software (Leica Geosystems Co., Ltd., Zurich, Switzerland). The error at each control point in the synthesized 3D coordinate dataset was adjusted to <2 mm. Vegetation points were manually removed from the merged 3D dataset. The processed 3D data were exported into ArcGIS and converted into a digital surface model dataset with a resolution of 1 cm (Fig. S2C). The digital surface model data were not interpolated because this could have introduced errors. Surface changes between the measurement campaigns were calculated.

2.4. Data analysis

The total ^{137}Cs activity (in Bq) was calculated by adding together the ^{137}Cs activities in the coarse and fine sediment samples. The ^{137}Cs concentration (in Bq kg^{-1}) was calculated by dividing the ^{137}Cs activity by the sediment mass. ^{137}Cs wash-off (in Bq m^{-2}) was calculated by multiplying the ^{137}Cs concentration in sediment by the amount of sediment discharged. A particle-size correction for the ^{137}Cs concentrations in particles of different sizes, determined from the particle size distribution, was applied to eliminate erratic variations caused by differences in particle sizes in the sediment samples (Wakiyama et al., 2019). In

previous studies, the ^{137}Cs concentration in sediment was found to be dependent on the particle size distribution (Walling and Woodward, 1992; Abril, 1996; He and Walling, 1996). This is caused by smaller particles having higher specific surface areas and therefore sorbing larger amounts of ^{137}Cs. We therefore calculated particle-size-corrected ^{137}Cs concentrations in the sediment samples using Eq. (1) to eliminate erratic variations caused by variations in the particle size distributions of the sediment samples, to allow temporal trends to be assessed.

$$C_{\text{correct}} = \frac{C}{P_{\text{correct}}} \quad (1)$$

In Eq. (1), C and C_{correct} are the observed ^{137}Cs concentration (Bq kg^{-1}) and the particle size-corrected ^{137}Cs concentration (Bq kg^{-1}), respectively, and $P_{correct}$ is the particle size correction factor (dimensionless), determined using the equation:

$$P_{\text{correct}} = \left(\frac{S_r}{S_s}\right)^{v} \quad (2)$$

where S_r is the specific surface area of the sediment sample (m^2 g^{-1}), S_s is the specific surface area of the standard sample (m^2 g^{-1}), and v is a constant. The specific surface area was estimated from the particle size distribution of the sample and a spherical approximation of particles in each size class. We used S_r and v values of 0.386 m^2 g^{-1} and 0.65, respectively, taken from a previous publication (Wakiyama et al., 2019).

Rainfall data were converted into an erosivity factor (R-factor; in MJ mm ha^{-1} h^{-1}) using the following equation:

$$R = \sum_{i=1}^{n} E_i I_{30i} \quad (3)$$

where E_i is the rainfall energy (MJ ha^{-1}) and I_{30i} is the maximum half-hour rainfall intensity (mm h^{-1}) for a storm (i).

Principal component analysis (PCA) was performed to assess the relationships between the topographic changes, ^{137}Cs concentrations, and relevant parameters (e.g., erosivity factors and sediment concentrations).

PCA was performed by using averaged or integrated observational data for each time point when ground surface changes were measured. Weighted mean values were used to calculate the ^{137}Cs concentration corrected for long-term decay (C_R), sediment concentration (C_S), the suspended sediment to total sediment ratio (C_{SS}), and discharge rate (R_Q). The integrated values were used to determine the R-factor (R). The total surface topography change (S_T) and rill area surface topography change (S_R), defined as the surface topography changes between consecutive observation times, were also taken into account. The effects of R, C_R, C_S, C_{SS}, R_Q, S_T, and S_R at each observation time were assessed by performing PCA.

Statistical analyses were performed in R 4.0.3 (R core team, 2020). Significant differences ($p < 0.05$) among the ^{137}Cs concentrations in in each of the three months were first examined via Kruskal-Wallis nonparametric ANOVA. Planned comparisons among the the ^{137}Cs concentrations were then conducted with Tukey-Kramer'stest ($p < 0.05$) to identify which ^{137}Cs concentrations differed from each other.

3. Results and discussion

3.1. Temporal variations in ^{137}Cs concentration and related variables

Temporal variations in (a) the accumulated rainfall (RF) and discharge rate (R_Q), (b) the total amount of washed-off sediment (T_S), (c) the sediment concentration (C_S), (c) the R-factor (R), (e) the suspended sediment to total sediment ratio (Css), (f) the particle size corrected ^{137}Cs concentration, and (g) the total surface topography change (S_T) at the experimental plot are shown in Fig. 2. A seasonal pattern, in which the amount of RF rises from spring to summer and then declines toward autumn, was confirmed for every year (Fig. 2a). The cumulative R_Q during the study period (Fig. 2a) showed similar seasonality. The T_S (sum of coarse/deposited and fine/suspended sediment) during the study period was also high from spring to autumn and decreased in winter (Fig. 2b). The C_S was relatively high in spring and started to decrease in the autumn (Fig. 2c). The seasonality of the R-factor was similar to RF (Fig. 2d). Vegetation cover generally decreases the sediment yield by mitigating the impact of raindrops on bare soil (Parsons et al., 1994 Parsons and Wainwright, 2006), on the other hand, it is considered that the high erosivity of rainfall during the summer could contribute the soil erosion on the controlled bare land. We found that the general decreasing trend in the particle size corrected ^{137}Cs concentration due to physical decay, downward migration, and surface wash-off (Fig. 2f). Here, environmental radiological decay was expressed using the exponential equation ($f = \alpha \exp[-(k_1 + \lambda)t]$), where λ ($=0.023$ yr^{-1}) is the physical decay constant of ^{137}Cs (half-life $= 30.1$ yr). The best-fitting values for parameters and k_1 were estimated as 30,125 (Bq kg^{-1}) and 0.270 (yr^{-1}), respectively. It was reported no clear temporal trends in the ^{137}Cs concentration in sediment in the first 2 yr after the FDNPP incident (Yoshimura et al., 2015), but we found a long-term decreasing trend in the ^{137}Cs concentration in transported sediment.

3.2. Seasonalilty in the ^{137}Cs concentration in washed-off sediment

Interestingly, the ^{137}Cs concentration in T_S was relatively low in winter and higher at other times. The ^{137}Cs concentration decreased from July 2012 to October 2012 but then increased markedly in April 2013. The ^{137}Cs concentration then decreased again after April 2013. A similar trend was found in 2014. The concentration of a radionuclide must, in principle, decrease because of physical decay and environmental redistribution. In previous studies, the ^{137}Cs concentration in transported sediment decreased as the particle size increased (Livens and Baxter, 1988 Walling and Quine, 1991). In another study, the ^{137}Cs concentration distribution decreased exponentially with soil depth (Takahashi et al., 2015). The ^{137}Cs concentration in T_S was expected to be strongly affected by (1) particle size effects caused by seasonality in the amounts of suspended and/or deposited sediment and (2) mixing and/or dilution by surface and relatively deep soil supplying the transported soil. If seasonal changes in the ^{137}Cs concentration were caused by seasonal changes in the sediment particle size distribution, particle size-correction of the ^{137}Cs concentrations using Eq. (1) would have removed the seasonality in the ^{137}Cs concentration. A seasonal trend was still found in the particle-size-corrected ^{137}Cs concentrations (Fig. S3). We therefore concluded that seasonality in the sediment particle size distribution was not the dominant factor causing seasonal changes in the ^{137}Cs concentration. Seasonality in the source of soil and in mixing of soil with relatively high and low ^{137}Cs concentrations would have led to seasonal changes in the ^{137}Cs concentration (Fig. 2f). The particle-size-corrected ^{137}Cs concentrations (later called simply ^{137}Cs concentrations) were used in the subsequent data analyses. Seasonal changes in the ground surface topography were found using the 3D scanning system (Fig. 2g). The ground surface was higher from fall (October 2012) to spring (March 2013) and lower during summer (March–July 2013). The amounts by which the surface became higher and lower were different in different years during the study, but clear seasonality was also observed between October 2013 and April 2014.

3.3. Seasonal changes in surface topography and the ^{137}Cs concentration

Particle size changes had only small effects on the seasonal trend in the ^{137}Cs concentration, meaning seasonal variations in the ^{137}Cs concentration were mainly caused by variations in the contributions of different sources of T_S (Fig. 3a). As mentioned above, the ^{137}Cs concentration will have decreased because of physical decay and environmental redistribution. However, both of the seasonal changes in the ^{137}Cs concentration

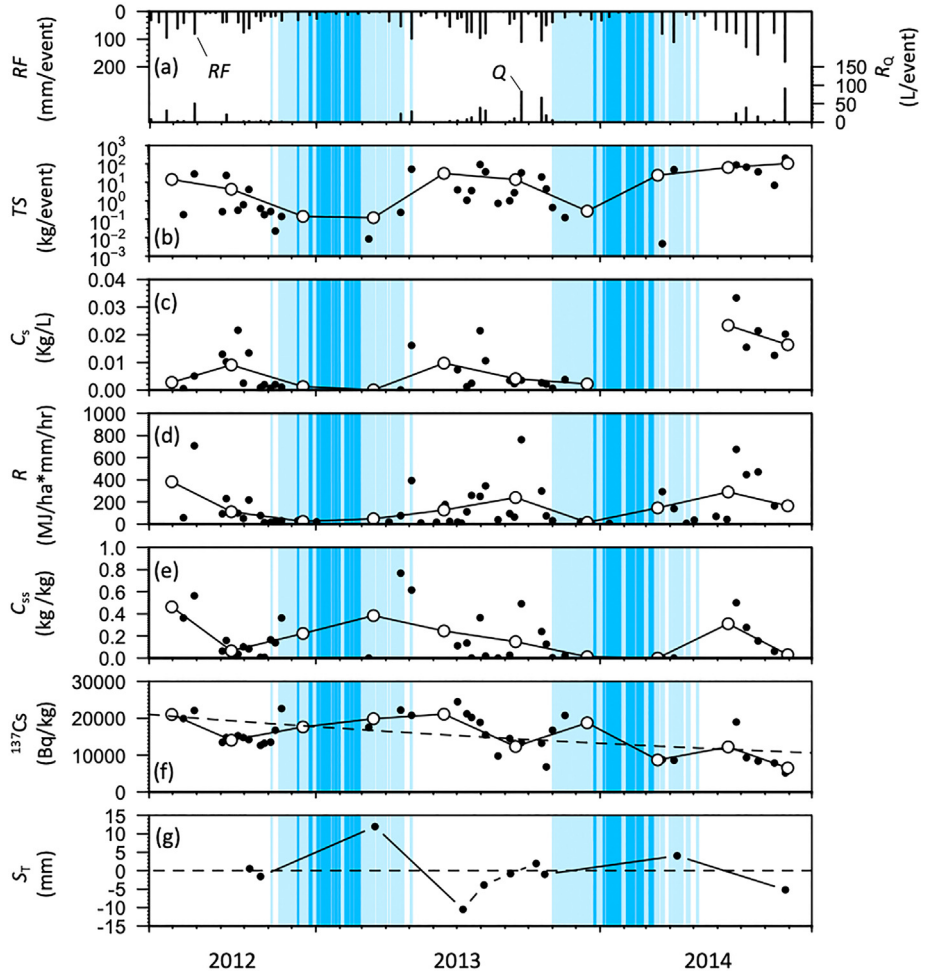

Fig. 2. Temporal variations in (a) the accumulated rainfall (*RF*) and discharge rate (R_Q), (b) the total amount of sediment transported (*TS*), (c) the sediment concentration (C_S), (c) the *R*-factor (*R*), (e) the suspended sediment to total sediment ratio (Css), (f) the ^{137}Cs concentration, and (g) the total surface topography change (S_T) at the experimental plot. The solid and empty circles indicate measured values and three-month averaged values, respectively. Dark blue and light blue indicate days when the daily average and minimum temperatures, respectively, were negative.

(Fig. 3a) and the ^{137}Cs concentrations corrected for long-term decay (Fig. 3b) were significantly different for the different phases (Tukye–Kramer's test, $p < 0.05$). The ^{137}Cs concentrations corrected for long-term decay were minimal in autumn and winter, and increases significantly in spring. The same trend was found throughout the 2 yr study period. Interestingly, seasonality in changes in the ^{137}Cs concentration was closely related to seasonality in S_T. We measured S_T using a 3D scanner to investigate seasonal variations in the sources of transported soil (Figs. S1 and S2). S_T at the experimental plot was divided into three phases (Fig. 3c). In phase 1, in autumn, the ^{137}Cs concentration was constant and minimal changes in the surface level occurred. In phase 2, in winter - spring, the ^{137}Cs concentration reached a minimum but then increased and the surface level gradually increased. In phase 3, in summer, the ^{137}Cs concentration and surface level decreased markedly.

3.3.1. Autumn

During the autumn season (Phase 1), the ^{137}Cs concentration was virtually constant, then the three-month average values were the lowest of all phases (Fig. 3a, b). In addition, there was little change on the ground surface during the phase 1 (Fig. 3c1–2, c6–8). The experimental plot, where soil surface was controlled as bare land, experienced several rainfall and wash-off events from spring to summer (Fig. 2a, b). These rainfall and wash-off events could have induced crusting and sealing at the soil surface (Nanko et al., 2008). Actually, we observed crusting and sealing at the soil surface during Phase 1 (Fig. 1c).

3.3.2. Winter and spring

During the winter-spring season (Phase 2), the ^{137}Cs concentration gradually increased (Fig. 3a; b) and then we also observed that the ground surface level increased (Fig. 3c3, c9). For instance, the whole ground surface, including the rill area, rose from 22 October 2012 to 18 March 2013 (Fig. 3c3). Then, the experimental plot experienced cold weather, which caused the ground surface to rise from freezing in winter to spring. Previous studies showed that the freeze-thaw processes produce unstable surface sediment during the cold season, such as late autumn and early spring, and can exert a significant influence on soil erosion as well as rainfall (Arnáez and Larrea, 1995; Arnáez et al., 2004 Bechmann et al., 2005 Nadal-Romero et al., 2008). Here, it is indeed assumed that the soil water transport of from the unfrozen (deep) layer to the frozen (surface) layer occurs due to the hydraulic potential by development of frost heaving under the freezing temperatures. Here it should be noted that the solid-liquid partition coefficient at Fukushima regions were reported as 1.43×10^5 to 1.65×10^6 (L/kg) (Taniguchi et al., 2019). This means that the^{137}Cs in soil is not easily soluble in water. Thus, water transport from the deep to the surface during the frost heaving may not contribute to the ^{137}Cs transport. The changes in ^{137}Cs concentration that remained would have been caused by ground surface changes during winter (when crusting and sealing of the soil surface caused during summer and fall (phase 1) would have been destroyed). It is considered that the freeze–thaw processes in winter and spring can supply the high ^{137}Cs concentration surface soil as an unstable sediment t on the ground surface. In addition, our site was

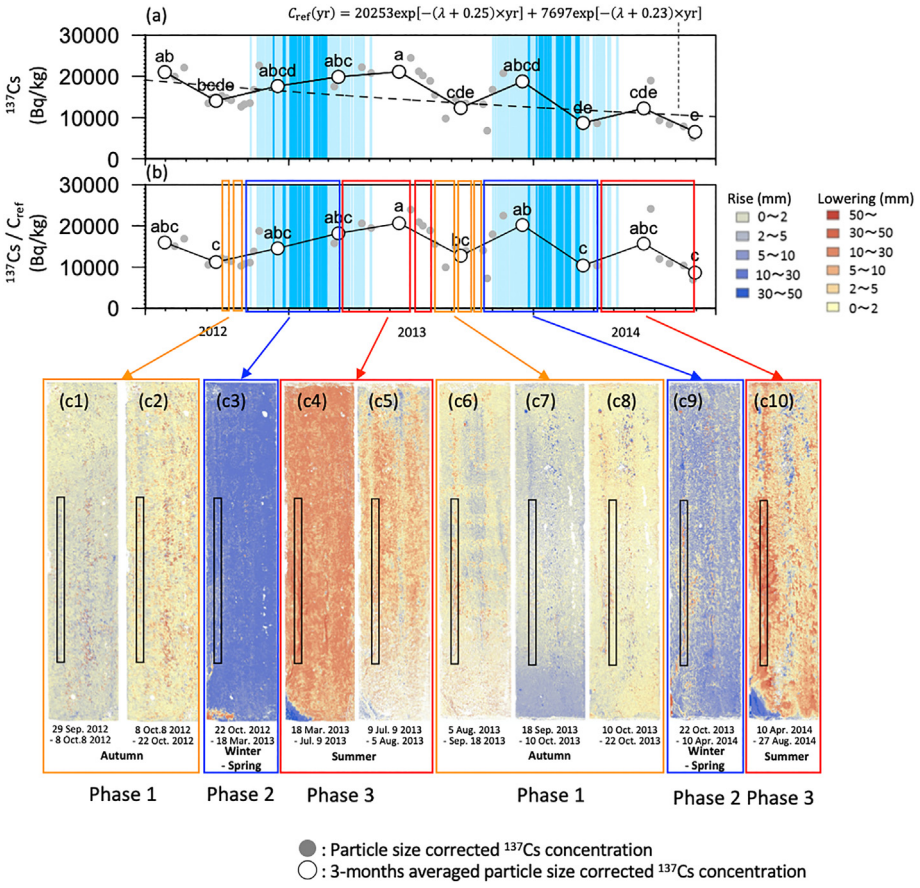

Fig. 3. (a) Particle size-corrected ^{137}Cs concentrations found at different times throughout the study. The solid and empty circles indicate the measured values and three-month averaged values, respectively. (b) Environmental decay collected (c) Topographic changes during phases 1, 2, and 3. The narrow black-edged areas indicate where rill erosion occurred.

controlled as a bare land and the ground surface was always exposed to the atmosphere. Thus, no-vegetated condition may have accelerated the crusting and sealing breakdown due to the freeze–thaw processes. Therefore, we concluded that freeze–thaw processes played important roles in creating unstable surface sediment with a relatively high ^{137}Cs concentration.

3.3.3. Summer

During the summer (Phase 3), soil surface was exposed summer time rainfall event (Fig. 3a; b), and high rainfall erosivity (Fig. 2d). These factors contributed to the down of whole ground surface and rill formation. Especially in the rill area, the decreasing of ground surface was larger than in other areas, indicating that the rill development for vertical direction (Fig. 3c4–5, c10). As shown in the previous study (Wakiyama et al., 2019), rill formation and the subsequent vertical rill expansion could provide a deeper soil which was less contaminated by accidentally released ^{137}Cs. When erosion progressed and the rill formation was started, the relatively deep and less contaminated soil was mixed in, and the ^{137}Cs concentration that washed-off also tended to decrease. Here, we would like to focus on the winter and summer of 2014. In this year, rainfall event in March and April just before the topographic measurement had started erosion processs, especially in the rill area. It is important to note that the heavy rainfall occurs in the early spring, caution is required because high concentrations of cesium may flow down into the river.

3.4. Factors controlling ^{137}Cs wash-off

Soil erosion and the ^{137}Cs concentration in the transported sediment would have been affected by various factors, such as the vegetation cover and land-use type (Nanko et al., 2008), rainfall intensity (Laceby et al., 2016), rill expansion (Gomi et al., 2008), and freeze–thaw processes (Bechmann et al., 2005; Nadal-Romero et al., 2008). PCA was therefore performed to assess the relationships between the wash-off event data and various factors that could have affected the wash-off event data. The effects of R, C_R, C_S, C_{SS}, R_Q, S_T, and S_R at each observation time were assessed by performing PCA (Fig. 4). The first two principal components could explain in total 76.9% of the variance with PC1 contributing with 53.2% and PC2 with 23.7%. Splitting the variables into 3-groups; one group (containing S_T and S_R) was on the left of, another group (containing R_Q, Cs, and Css) was in the upper right of, and the third group (containing R and C_R) was in the lower right. Observations 4 and 5 (in the upper right of Fig. 4) were made in a period (spring and summer, 18 March 13 to 9 July 2013) in which the ground surface became markedly lower (Fig. 3c4 and c5), and both the sediment and suspended sediment concentrations decreased (Fig. 2e and f). This indicated that unstable sediment on the ground surface was eroded because of freeze–thaw in winter and spring. The ^{137}Cs concentration started to increase in March 2013 after a rainfall event, reached a maximum in July 2013, and then started to decrease (Fig. 3a and b). Almost the same processes were assumed to have occurred for observation 10, which was characterized by R and C_S (in the lower right of Fig. 4). Interestingly, the PCA results indicated that winter and spring (observations 3 and 9) were characterized by surface changes occurring (on the left in Fig. 4) because of freeze–thaw processes occurring in the winter. It should be noted that the effects of surface changes on observation 9 may not have been noticeable because of a discharge event (Fig. 2b) and rill formation (Fig. 3b9) caused by rainfall in late March 2014 (Fig. 2a). The PCA results indicated that winter (when freeze–thaw processes occurred) was distinguished from the other seasons because of surface changes. (See Fig. 3c.)

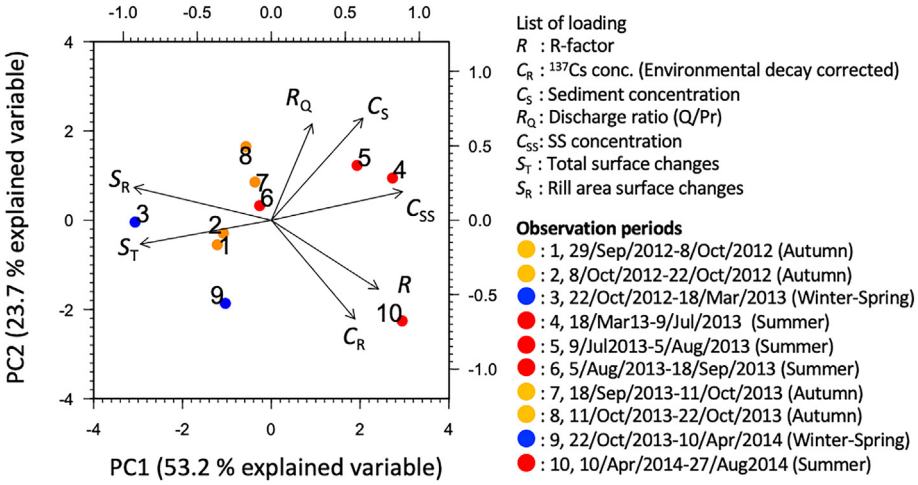

Fig. 4. Principal component analysis results for the ^{137}Cs concentrations and other variables.

3.5. What does the seasonality of ^{137}Cs concentrations mean for the surrounding environment?

This study revealed that ^{137}Cs concentrations of washed-off sediments from the bare land varied seasonally and that freeze-thaw processes on the soil surface contributed to the seasonal variation (see Fig. 5). A current review study (Onda et al., 2020) points out the importance of particulate radio cesium transport from rivers to the sea in Fukushima. Cesium discharged from bare land is assumed to be the source of cesium in particulate transported in rivers. For example, radiocesium concentrations in riverine sediment in downstream areas have been found to increase after large discharge events such as typhoons (Nagao et al., 2013). Therefore, if a similar number of rainfall events occurs, it could be assumed that ^{137}Cs concentrations in riverine sediment and therefore ^{137}Cs fluxes to the marine environment will be higher (and therefore ^{137}Cs effects on the marine environment will be more severe) in winter and spring (when surface soil has been affected by freeze–thaw processes) than in summer and fall. For example, ^{137}Cs in particulates transported from rivers to the sea has been found to be the source of dissolved ^{137}Cs in coastal/nearshore seawater (Takata et al., 2016, 2020). Marine fish have been found to take up dissolved ^{137}Cs released from particulate-bound ^{137}Cs supplied by rivers to the sea, but the ^{137}Cs concentrations marine fish were not found to vary seasonally (Tagami and Uchida, 2016). Seasonal changes in particulate-bound ^{137}Cs concentrations in river sediment will

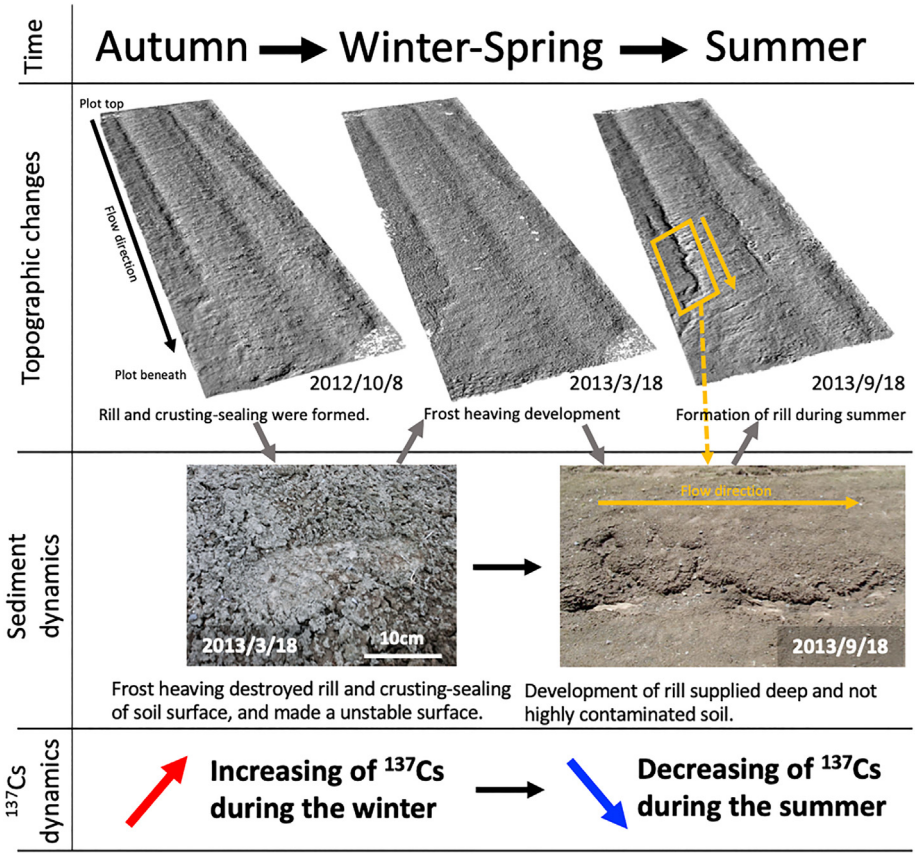

Fig. 5. Schematic illustration of the observed changes in surface topography, sediment dynamics, and ^{137}Cs concentrations in washed-off sediment.

very strongly affect ^{137}Cs transfer to freshwater fish. In fact, seasonal changes in ^{137}Cs concentrations in freshwater fish have been found (Wada et al., 2016). Interactions between particulate-bound ^{137}Cs concentrations in river sediment and ^{137}Cs concentrations in freshwater fish need to be studied further. Seasonality in ^{137}Cs concentrations, particularly in sediment eroded from slopes, should be considered in future studies of the transport of ^{137}Cs attached to suspended sediment in rivers to the sea.

4. Conclusion

This is the first study of the effects of freeze–thaw processes and subsequent runoff on ^{137}Cs fluxes and concentrations in sediment discharged from a bare land erosion plot after the FDNPP accident. We found a general decrease in the particle-size-corrected ^{137}Cs concentration caused by physical decay, downward migration, and surface washoff. The particle-size-corrected ^{137}Cs concentration was relatively low in winter and higher in the other seasons. The 3D scanning results indicated that freeze–thaw processes played important roles in the production of unstable surface sediment (which had a relatively high ^{137}Cs concentration after winter) and that rill incision increased sediment discharges from subsurface soil layers and decreased the ^{137}Cs concentration in the eroded sediment from spring to fall. Seasonal changes in the ^{137}Cs concentration were strongly controlled by the changes in the source (surface or deeper soil) of the eroded soil, which are controlled by freeze–thaw processes and rill formation. This must be taken into account when modeling radionuclide wash-off.

Funding sources

This work is also supported by JSPS KAKENHI (Grant numbers: 24110006).

Science and Technology Research Partnership for Sustainable Development JST-JICA, Japan (SATREPS project; PI. Kenji Nanba; JPMJSA1603).

CRediT authorship contribution statement

Yasunori Igarashi: Writing – original draft, Formal analysis. **Yuichi Onda:** Writing – original draft, Formal analysis. **Yoshifumi Wakiyama:** Formal analysis, Investigation, Resources. **Kazuya Yoshimura:** Investigation, Resources. **Hiroaki Kato:** Investigation, Resources. **Shohei Kozuka:** Investigation, Resources. **Ryo Manome:** Investigation, Resources.

Declaration of competing interest

The authors declare that they have no known competing financial interests or personal relationships that could have appeared to influence the work reported in this paper.

Acknowledgements

This work was funded by the Japanese Ministry of Education, Culture, Sports, Science and Technology (FY2011-2012) and the Nuclear Regulation Authority of Japan (FY 2012–2014). This work was also supported through a Grant-in-Aid for Scientific Research on Innovative Areas (grant number 24110006) and the Japanese government (JST/JICA) program for international joint research into global issues, called the Science and Technology Research Partnership for Sustainable Development JST-JICA, Japan (SATREPS project; PI. Kenji Nanba; grant number JPMJSA1603). We thank Gareth Thomas, PhD, from Edanz Group (www.edanzediting.com/ac) for editing a draft of this manuscript.

Appendix A. Supplementary data

Supplementary data to this article can be found online at https://doi.org/10.1016/j.scitotenv.2020.144706.

References

Abril, J.M., 1996. Some physical and chemical features of the variability of K_d distribution coefficients for radionuclides. Fuel. Energy. Abstr. 37, 308. https://doi.org/10.1016/0140-6701(96)82745-7.

Arnáez, J., Larrea, V., 1995. Erosion processes and rates on road-sides of hill-roads (Iberian System, La Rioja, Spain). Phys. Chem. Earth 20, 395–401. https://doi.org/10.1016/0079-1946(95)00053-4.

Arnáez, J., Larrea, V., Ortigosa, L., 2004. Surface runoff and soil erosion on unpaved forest roads from rainfall simulation tests in northeastern Spain. Catena 57, 1–14. https://doi.org/10.1016/j.catena.2003.09.002.

Bechmann, M.E., Kleinman, P.J.A., Sharpley, A.N., Saporito, L.S., 2005. Freeze-thaw effects on phosphorus loss in runoff from manured and catch-cropped soils. J. Environ. Qual. 34, 2301–2309. https://doi.org/10.2134/jeq2004.0415.

Beresford, N.A., Fesenko, S., Konoplev, A., Skuterud, L., Smith, J.T., Voigt, G., 2016. Thirty years after the Chernobyl accident: what lessons have we learnt? J. Environ. Radioact. 157, 77–89. https://doi.org/10.1016/j.jenvrad.2016.02.003.

Bulgakov, A.A., Konoplev, A.V., Popov, V.Y., Shcherbak, A.V., 1991. Removal of long-lived radionuclides from the soil by surface runoff near the Chernobyl Nuclear Power Station. Sov. Soil Sci. Pochvovedeniye 23, 124–131.

Bulgakov, A.A., Konoplev, A.V., Shveikin, Y.V., Scherbak, A.V., 1999. Experimental study and prediction of dissolved radionuclide wash-off by surface runoff from non-agricultural watersheds. Contaminated Forests. Springer Netherlands, Dordrecht, pp. 103–112 https://doi.org/10.1007/978-94-011-4694-4_11.

Carvalho, F.P., 2018. Radionuclide concentration processes in marine organisms: a comprehensive review. J. Environ. Radioact. 186, 124–130. https://doi.org/10.1016/j.jenvrad.2017.11.002.

Eltner, A., Baumgart, P., 2015. Accuracy constraints of terrestrial Lidar data for soil erosion measurement: application to a Mediterranean field plot. Geomorphology 245, 243–254. https://doi.org/10.1016/j.geomorph.2015.06.008.

Eltner, A., Baumgart, P., Maas, H.G., Faust, D., 2015. Multi-temporal UAV data for automatic measurement of rill and interrill erosion on loess soil. Earth Surf. Process. Landf. 40, 741–755. https://doi.org/10.1002/esp.3673.

Garcia-Sanchez, L., Konoplev, A., Bulgakov, A., 2005. Radionuclide entrainment coefficients by wash-off derived from plot experiments near Chernobyl. Radioprotection 40, S519–S524. https://doi.org/10.1051/radiopro:2005s1-076.

Garcia-Sanchez, L., Konoplev, A.V., 2009. Watershed wash-off of atmospherically deposited radionuclides: a review of normalized entrainment coefficients. J. Environ. Radioact. 100, 774–778. https://doi.org/10.1016/j.jenvrad.2008.08.005.

Gomi, T., Sidle, R.C., Miyata, S., Kosugi, K., Onda, Y., 2008. Dynamic runoff connectivity of overland flow on steep forested hillslopes: scale effects and runoff transfer. Water Resour. Res. 44, 1–16. https://doi.org/10.1029/2007WR005894.

Haubrock, S.N., Kuhnert, M., Chabrillat, S., Güntner, A., Kaufmann, H., 2009. Spatiotemporal variations of soil surface roughness from in-situ laser scanning. Catena 79, 128–139. https://doi.org/10.1016/j.catena.2009.06.005.

He, Q., Walling, D.E., 1996. Interpreting particle size effects in the adsorption of ^{137}Cs and unsupported ^{210}Pb by mineral soils and sediments. J. Environ. Radioact. 30, 117–137. https://doi.org/10.1016/0265-931X(96)89275-7.

Jester, W., Klik, A., 2005. Soil surface roughness measurement - methods, applicability, and surface representation. Catena 64, 174–192. https://doi.org/10.1016/j.catena.2005.08.005.

Konoplev, A.V., Bulgakov, A.A., Popov, V.E., Bobovnikova, T.I., 1992. Behaviour of long-lived Chernobyl radionuclides in a soil-water system. Analyst 117, 1041–1047. https://doi.org/10.1039/an9921701041.

Konoplev, A.V., Bulgakov, A.A., Popov, V.E., Popov, O.F., Scherbak, A.V., Shveikin, YuV, Hoffman, F.O., 1996. Model testing using Chernobyl data: I. Wash-off of ^{90}Sr and ^{137}Cs from two experimental plots established in the vicinity of the Chernobyl reactor. Health Phys. 70, 8–12.

Laceby, J.P., Chartin, C., Evrard, O., Onda, Y., Garcia-Sanchez, L., Cerdan, O., 2016. Rainfall erosivity in catchments contaminated with fallout from the Fukushima Daiichi nuclear power plant accident. Hydrol. Earth Syst. Sci. 20, 2467–2482. https://doi.org/10.5194/hess-20-2467-2016.

Livens, F.R., Baxter, M.S., 1988. Particle size and radionuclide levels in some west Cumbrian soils. Sci. Total Environ. 70, 1–17. https://doi.org/10.1016/0048-9697(88)90248-3.

MEXT (Ministry of Education, Culture, Sports, Science and Technology), 2011. Results of the Third Airborne Monitoring Survey by MEXT. http://radioactivity.nsr.go.jp/ja/contents/5000/4858/24/1305819_0708.pdf. (Accessed 9 November 2020).

Nadal-Romero, E., Latron, J., Martí-Bono, C., Regüés, D., 2008. Temporal distribution of suspended sediment transport in a humid Mediterranean badland area: the Araguás catchment, Central Pyrenees. Geomorphology 97, 601–616. https://doi.org/10.1016/j.geomorph.2007.09.009.

Nagao, S., Kanamori, M., Ochiai, S., Tomihara, S., Fukushi, K., Yamamoto, M., 2013. Export of ^{134}Cs and ^{137}Cs in the Fukushima river systems at heavy rains by Typhoon Roke in September 2011. Biogeosciences 10, 6215–6223. https://doi.org/10.5194/bg-10-6215-2013.

Nakao, A., Ogasawara, S., Sano, O., Ito, T., Yanai, J., 2014. Radiocesium sorption in relation to clay mineralogy of paddy soils in Fukushima, Japan. Sci. Total Environ. 468–469, 523–529. https://doi.org/10.1016/j.scitotenv.2013.08.062.

Nanko, K., Mizugaki, S., Onda, Y., 2008. Estimation of soil splash detachment rates on the forest floor of an unmanaged Japanese cypress plantation based on field measurements of throughfall drop sizes and velocities. Catena 72, 348–361. https://doi.org/10.1016/j.catena.2007.07.002.

Obara, H., Okura, T., Takata, Y., Kohyama, K., Maejima, Y., Hamazaki, T., 2011. Bulletin of National Institute for Agro-Environmental Sciences No. 29. https://doi.org/10.24514/00002990.

Onda, Y., Taniguchi, K., Yoshimura, K., Kato, H., Takahashi, J., Wakiyama, Y., Coppin, F., Smith, H., 2020. Radionuclides from the Fukushima Daiichi Nuclear Power Plant in terrestrial systems. Nature Rev. Earth Environ. 1. https://doi.org/10.1038/s43017-020-0099-x.

Parsons, A.J., Abrahams, A.D., Wainwright, J., 1994. Rainsplash and erosion rates in an interrill area on semi-arid grassland, Southern Arizona. Catena 22, 215–226. https://doi.org/10.1016/0341-8162(94)90003-5.

Parsons, A.J., Wainwright, J., 2006. Depth distribution of interrill overland flow and the formation of rills. Hydrol. Process. 20, 1511–1523. https://doi.org/10.1002/hyp.5941.

Peel, M.C., Finlayson, B.L., McMahon, T.A., 2007. Updated world map of the Köppen-Geiger climate classification. Hydrol. Earth Syst. Sci. 11, 1633–1644. https://doi.org/10.5194/hess-11-1633-2007.

R Core Team, 2020. A Language and Environment for Statistical Computing. R Foundation for Statistical Computing, Vienna, Austria 3-900051-07-0 URL, http://www.R-project.org.

Sansone, U., Bellia, M., Voitsekovitchb, O.V., Kanivetsb, V., 1996. ^{137}Cs and ^{90}Sr in water and suspended particulate matter of the Dnieper River-Reservoirs System (Ukraine). Sci. Total Environ. 186, 257–271. https://doi.org/10.1016/0048-9697(96)05120-0.

Santschi, P.H., Bollhalder, S., Farrenkothen, K., Lueck, A., Zlngg. S., Sturm, M., 1988. Chernobyl radionuclides in the environment: tracers for the tight coupling of atmospheric, terrestrial, and aquatic geochemical processes. Environ. Sci. Technol. 22, 510–516. https://doi.org/10.1021/es00170a004.

Santschi, P.H., Bollhalder, S., Zingg, S., Lück, A., Farrenkothen, K., 1990. The self-cleaning capacity of surface waters after radioactive fallout. Evidence from European Waters after Chernobyl, 1986–1988. Environ. Sci. Technol. 24, 519–527. https://doi.org/10.1021/es00074a009.

Smith, J., Beresford, N.A., 2005. Chernobyl — Catastrophe and Consequences. Springer, Springer Praxis Books. Springer Berlin Heidelberg https://doi.org/10.1007/3-540-28079-0.

Steinhauser, G., Brandl, A., Johnson, T.E., 2014. Comparison of the Chernobyl and Fukushima nuclear accidents: a review of the environmental impacts. Sci. Total Environ. 470–471, 800–817. https://doi.org/10.1016/j.scitotenv.2013.10.029.

Tagami, K., Uchida, S., 2016. Consideration on the long ecological half-life component of ^{137}Cs in demersal fish based on field observation results obtained after the Fukushima accident. Environ. Sci. Technol. 50, 1804–1811. https://doi.org/10.1021/acs.est.5b04952.

Takahashi, J., Tamura, K., Suda, T., Matsumura, R., Onda, Y., 2015. Vertical distribution and temporal changes of ^{137}Cs in soil profiles under various land uses after the Fukushima Dai-ichi Nuclear Power Plant accident. J. Environ. Radioact. 139, 351–361. https://doi.org/10.1016/j.jenvrad.2014.07.004.

Takata, H., Kusakabe, M., Inatomi, N., Ikenoue, T., Hasegawa, K., 2016. The contribution of sources to the sustained elevated inventory of ^{137}Cs in offshore waters East of Japan after the Fukushima Dai-ichi nuclear power station accident. Environ. Sci. Technol. 50 (13), 6957–6963. https://doi.org/10.1021/acs.est.6b00613.

Takata, H., Inatomi, N., Kudo, N., 2020. The contribution of ^{137}Cs export flux from the Tone River Japan to the marine environment. Sci. Total Environ. 701, 134,550. https://doi.org/10.1016/j.scitotenv.2019.134550.

Taniguchi, K., Onda, Y., Smith, H.G., Blake, W., Yoshimura, K., Yamashiki, Y., Kuramoto, T., Saito, K., 2019. Transport and Redistribution of Radiocesium in Fukushima Fallout through Rivers. Environ. Sci. Technol. 53, 12,339–12,347. https://doi.org/10.1021/acs.est.9b02890.

Wada, T., Tomiya, A., Enomoto, M., Sato, T., Morishita, D., Izumi, S., Niizeki, K., Suzuki, S., Morita, T., Kawata, G., 2016. Radiological impact of the nuclear power plant accident on freshwater fish in Fukushima: an overview of monitoring results. J. Environ. Radioact. 151, 144–155. https://doi.org/10.1016/j.jenvrad.2015.09.017.

Wakiyama, Y., Onda, Y., Yoshimura, K., Igarashi, Y., Kato, H., 2019. Land use types control solid wash-off rate and entrainment coefficient of Fukushima-derived ^{137}Cs, and their time dependence. J. Environ. Radioact. 105, 990. https://doi.org/10.1016/j.jenvrad.2019.105990.

Walling, D.E., Quine, T.A., 1991. Use of ^{137}Cs measurements to investigate soil erosion on arable fields in the UK: potential applications and limitations. J. Soil Sci. 42, 147–165. https://doi.org/10.1111/j.1365-2389.1991.tb00099.x.

Walling, D.E., Woodward, J.C., 1992. Use of radiometric fingerprints to derive information on suspended sediment sources. Eros. Sediment Monit. Program. River Basins. Proc. Int. Symp. Oslo. 1992, pp. 153–164.

Yoshimura, M., Akama, A., 2014. Radioactive contamination of aquatic insects in a stream impacted by the Fukushima nuclear power plant accident. Hydrobiologia 722, 19–30. https://doi.org/10.1007/s10750-013-1672-9.

Yoshimura, K., Onda, Y., Kato, H., 2015. Evaluation of radiocaesium wash-off by soil erosion from various land uses using USLE plots. J. Environ. Radioact. 139, 362–369. https://doi.org/10.1016/j.jenvrad.2014.07.019.